DOI 10.3233/JAE-2010-1165
IOS Press

A study of inductance displacement sensor on optical aperture synthesistelescope

Haitao Wang[a,*], Qiufeng Luo[a], Jiahui Cai[a], Yajing Zhang[a], Junwei Wan[a], Yongkai Zhu[a] and Gui Yun Tian[a,b]
[a]*School of Automation Engineering, Nanjing University of Aeronautics and Astronautics, Nanjing, Jiangsu, 210016, P.R. China*
[b]*University of Newcastle upon Tyne, NE 7RU, UK*

Abstract. The principle of the inductance displacement sensor on optical aperture synthesis telescope is given with a measurement of mutual inductance to deduce the axial distance. It illustrates an effective modelling and calculation method based on Partial Element Equivalent Circuit (PEEC). PEEC is the method to calculate mutual inductances between coils utilizing partial parameter concept. Simulation for the change of mutual inductances is done which is prepared for the next step work.

Keywords: Optical aperture synthesis, mutual inductance, displacement sensor

1. Introduction

Optical aperture synthesis (OAS) technology [1,2] is a kind of process technology which joints available small diameter mirrors to form a large diameter telescope. Specifically, it is a technology of arranging, supporting, detecting and controlling several small diameter sub-mirrors, which can work equivalently as a bigger diameter telescope, and obtains high resolution observation.

One of the key techniques for the OAS telescope is how to maintain each sub-aperture mirror surface's position, or how to detect and control each sub-mirror co-focus and co-phase. Nowadays, there are three types of displacement sensors successfully implicated in the segmented mirrors [3]: the capacitance type, the inductance type and the photoelectricity type. Emphasis is placed on the inductance displacement sensor in this paper whose advantages are smaller volume, lighter weight and the reasonable price.

Figure 1 shows sensor geometry for differential distance measurement [4]. The sensor requires that pairs of inductors be installed on the opposite edges of the neighbouring segments. One pair of these inductors is referred to as the "Passive" side since it doesn't require power and is not physically connected to the other pair which is referred to as the "Active" side. These two pairs of coils, or the active and passive sides of the sensor, are separated by the gap between adjacent segments. They are located on the opposing faces of these segments such that they are geometrically opposite to each other when the two segments are properly aligned. Flat spiral wound coils on the active side couple inductively to identical coils on the passive side.

*Corresponding author: Haitao Wang, School of Automation Engineering, Nanjing University of Aeronautics and Astronautics, Nanjing, Jiangsu, 210016, P.R. China. Tel.: +86 2584896264; E-mail: htwang@nuaa.edu.cn, whtlqf@hotmail.

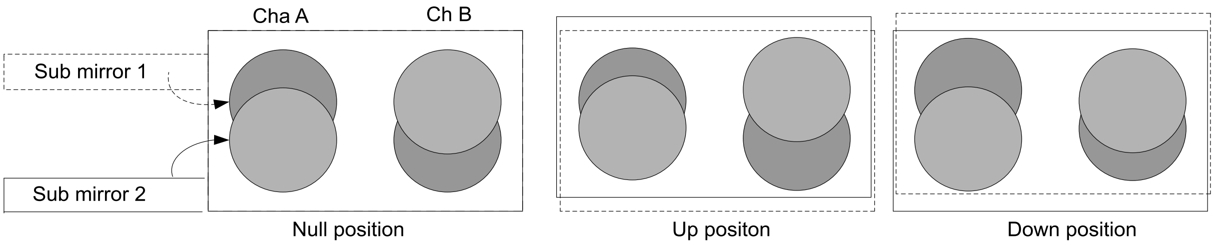

Fig. 1. Coils geometry for differential distance measurement.

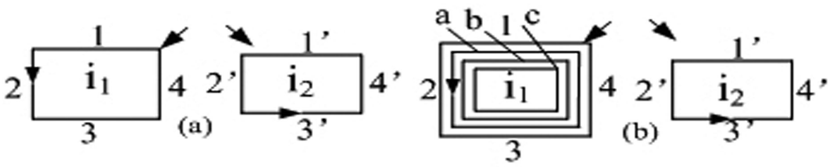

Fig. 2. Schematic diagram for the principle of PEEC.

The principle of inductance type is: once the mirror migrates from a particular position, the axial distance of the coils can be deduced from the change in mutual inductance(impedance change in coils) coursed by the movement of the coils installed at the edge of neighboring mirror surfaces (as shown in Fig. 1).

Based on experiments about the model and the position of coils, this paper using flat spiral polygon coils approaching circular spiral coils, simulated the mutual inductance changes of coils caused by the coil migration, using partial parameter concept as well as subdivision principle of PEEC. So that the quantity changes of the coil mutual inductance caused by the corresponding displacement change can be obtained, which would be proved in the following work by designing the examination system.

2. Mutual inductance calculation based on PEEC

The mutual inductance between the loops depends on the coils shape, spatial location and current distribution in the wire, which is often calculated according the Formula Neumann. However, use of analytical formulas to calculate mutual inductance is not suitable any more in cases if the shape of wire is rather complicated or if the current distribution in wire is non-uniform because of eddy effect. Finite element method [5] can accurately model the irregular wire, and calculate the effect of eddy exactly, but it isn't a smart enough to calculate the three-dimensional open-domain model for the reason that the work load for finite element modelling and calculating is huge. It is an effective method to use PEEC [6] to calculate the mutual inductance which is numerical computation method through partial parameters and partition.

$$M = \sum_{i=1}^{4} M_{i1'} + \sum_{i=1}^{4} M_{i2'} + \sum_{i=1}^{4} M_{i3'} + \sum_{i=1}^{4} M_{i4'} = \sum_{i=1}^{4} \sum_{j=1}^{4'} M_{ij} \tag{1}$$

Figure 2 briefly illustrates the principle of calculation between coils based on PEEC. As showed in Fig. 2(a), two filaments consist of two rectangular loop i1 and i2 (can be equivalent for the current

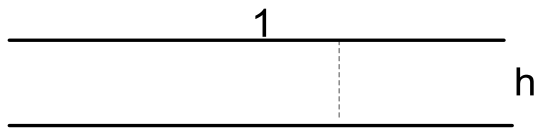

Fig. 3. Two parallel equilong lines.

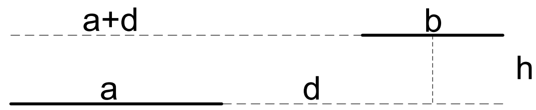

Fig. 4. Two parallel straight lines in general case.

filaments), each loop consists of four straight lines. According to PEEC theory, there is partial mutual inductance between every two straight lines. Therefore, mutual inductance could be obtained through summing up the total partial mutual inductances.

Regarding quite complex wire situation, for example, the left figure of Fig. 2(b), the rectangular coil formation could be subdivided into some similar current filaments loop as the chart a, b and c show. The current in every filament is part of total current through the wire, so the mutual inductance of entire loop i1 and i2 could be calculated by the Formula Eq. (2).

$$M = \frac{i_a}{i_1}M_a + \frac{i_b}{i_1}M_b + \frac{i_c}{i_1}M_c \tag{2}$$

Where Ma, Mb and Mc are the mutual inductances among filaments a, b, c and filament i2 respectively, could be calculated by the formula Eq. (1). i_a, i_b and i_c are the current through each filament. Obviously, through appropriate subdivision and calculation of the partial mutual inductance on complex wire, finally the mutual inductance can be obtained by summing up the partial mutual inductances. In order to guarantee that the current of filaments are equal, it is requested that subdivision needs to defer to the actual current distribution. What's more, thinner the filament is, smaller the error become. The analysis formulas [7] are used to approximately calculate partial mutual inductances.

Calculation formulas for different situations are given below.

1. Figures 3 and 4 show the two statements of parallel straight lines.
   Calculation formula for two parallel equilong lines is given as Eq. (3):
   $$M = \frac{\mu_0 l}{2\pi}\left[\ln\left(\frac{l+\sqrt{l^2+h^2}}{h}\right) - \frac{\sqrt{l^2+h^2}}{h} + \frac{h}{l}\right] \tag{3}$$
2. Calculation formula for two parallel straight lined in general case (as shown in Fig. 4) is given as Eq. (4):
   $$\begin{aligned} M = \frac{\mu_0}{4\pi}[&\alpha\ln(\alpha+\sqrt{\alpha^2+h^2}) - \beta\ln(\beta+\sqrt{\beta^2+h^2}) - \gamma\ln(\gamma+\sqrt{\gamma^2+h^2}) + \\ &\delta\ln(\delta+\sqrt{\delta^2+h^2}) - \sqrt{\alpha^2+h^2} + \sqrt{\beta^2+h^2} + \sqrt{\gamma^2+h^2} - \sqrt{\delta^2+h^2}] \end{aligned} \tag{4}$$
   where $\alpha + a + d + b; \beta = a + d; \gamma = b + d; \delta = d;$
3. Figure 5 shows the situation where two lines which are unparallel in a plane. The formula in this situation is given in Eq. (5).
   $$M = \frac{\mu_0}{2\pi}\cos\varphi \times \left(x_2 Arth\frac{b}{D_{22}+D_{21}} + y_2 Arth\frac{a}{D_{22}+D_{21}} - \right.$$

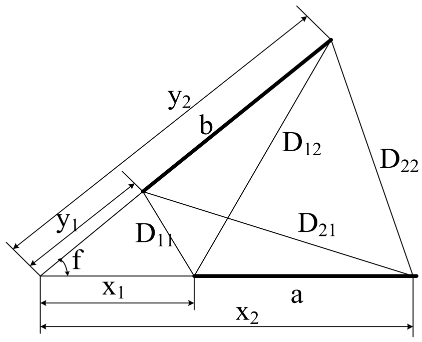

Fig. 5. Two lines which are unparallel in a plane.

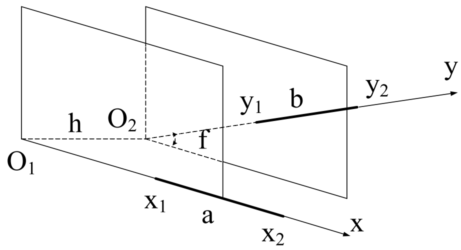

Fig. 6. Two lines in general case.

$$x_1 Arth\frac{b}{D_{11}+D_{12}} - y_1 Arth\frac{a}{D_{11}+D_{12}}\Bigg) \tag{5}$$

Where D_{11}, D_{12}, D_{21}, D_{22} represent the distances shown in Fig. 5:

$$D_{11}^2 = x_1^2 + y_1^2 - 2x_1y_1\cos\varphi \tag{6}$$

$$D_{12}^2 = x_1^2 + y_2^2 - 2x_1y_2\cos\varphi \tag{7}$$

$$D_{21}^2 = x_2^2 + y_1^2 - 2x_2y_1\cos\varphi \tag{8}$$

$$D_{22}^2 = x_2^2 + y_2^2 - 2x_2y_2\cos\varphi \tag{9}$$

4. Two lines in general case. As shown in Fig. 6, two parallel plates could always be found in which containing two lines in general case (as shown in Fig. 6). φ is the Included angle between lines ($0 \leqslant \varphi \leqslant \pi$); x and y is the axial of coordinate; x1, x2, y1, y2 are the beginning and terminal coordinates of the wire; D_{11}, D_{12}, D_{21}, D_{22} are the distances between the corrdinates.

$$\begin{aligned} M = \frac{\mu_0}{2\pi}\cos\varphi \times \Bigg(& x_2 Arth\frac{b}{D_{22}+D_{21}} + y_2 Arth\frac{a}{D_{22}+D_{21}} - \\ & x_1 Arth\frac{b}{D_{11}+D_{12}} - y_1 Arth\frac{a}{D_{11}+D_{12}} + \frac{h}{\sin\varphi}A\Bigg) \end{aligned} \tag{10}$$

where

$$A = arctg\left(\frac{x_1+y_1+D_{11}}{h}tg\frac{\varphi}{2}\right) + arctg\left(\frac{x_2+y_2+D_{22}}{h}tg\frac{\varphi}{2}\right) - \tag{11}$$

Table 1
Legnth of outmost side in different geomety

Geomety	Dimension
Quadrilateral spiral coils	20 mm
Hexagonal spiral coils	10 mm
Octagonal sprial coils	12 mm
Dodecagonal sprial coils	7.5 mm

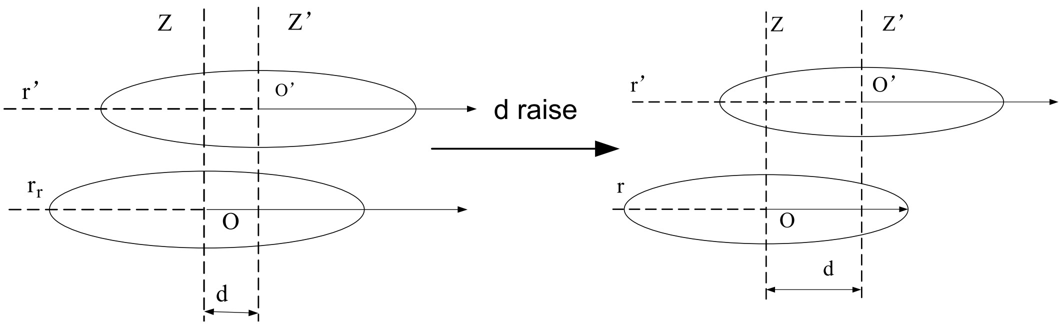

Fig. 7. Another view of the coils construction.

$$arctg\left(\frac{x_1+y_2+D_{12}}{h}tg\frac{\varphi}{2}\right)-arctg\left(\frac{x_2+y_1+D_{21}}{h}tg\frac{\varphi}{2}\right)$$

$$D_{11}^2=x_1^2+y_1^2-2x_1y_1\cos\varphi+h^2 \tag{12}$$

$$D_{12}^2=x_1^2+y_2^2-2x_1y_2\cos\varphi+h^2 \tag{13}$$

$$D_{21}^2=x_2^2+y_1^2-2x_2y_1\cos\varphi+h^2 \tag{14}$$

$$D_{22}^2=x_2^2+y_2^2-2x_2y_2\cos\varphi+h^2 \tag{15}$$

3. Simulation example

As the demand of the sensor system, the flat circular spiral wound coils whose size is at millimetre magnitude are preferred. Figure 7 is anther view of the coils construction when the coaxial distance d is changed.

We know that, in theory, when the number of a polygon's sides tends to infinity, the polygon is equal to a circle. In this paper, spiral polygon is used to approach spiral circle through increasing the number of polygon edges gradually. We supposed that the current density in lines is equal. So, the filamants are equally subdivided in a line. By using the equations metioned above, the mutual inductance between two spiral polygon coils can be calculated. Thus, the mutual inductance between two spiral circle wound coils at different coaxial distance is approached by a polygon with the certain number sides.

A simulation example is given here to evalute the validity of the method. The primary and secondary coils are indentical. The geogetric and characteristic parameters of the spiral coils are given: copper track width is 0.2 mm, copper track separation is 0.5 mm and number of turns is 8. And legnth of outer most side in different geomety are given in Table 1.

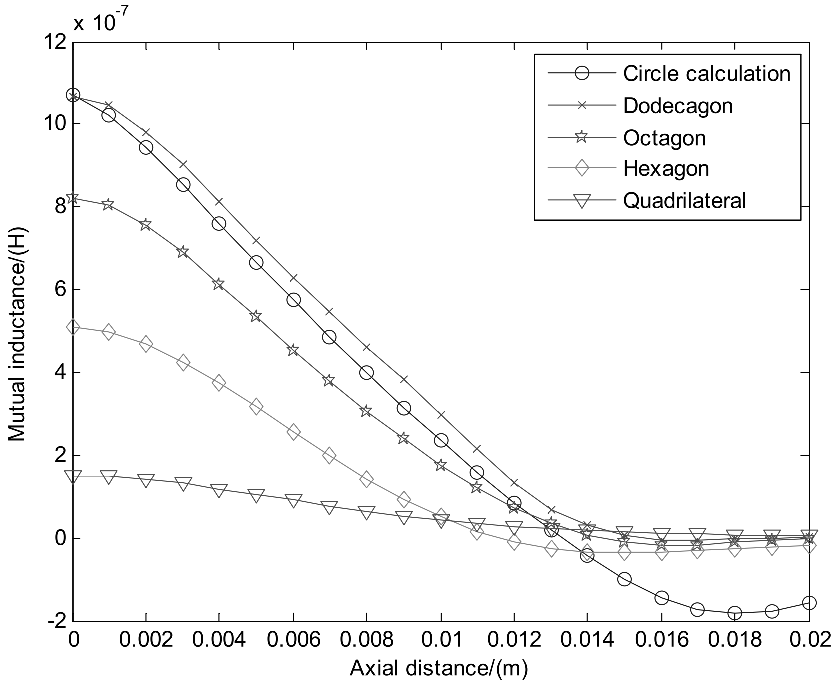

Fig. 8. Mutual inductance as a function of axial distance.

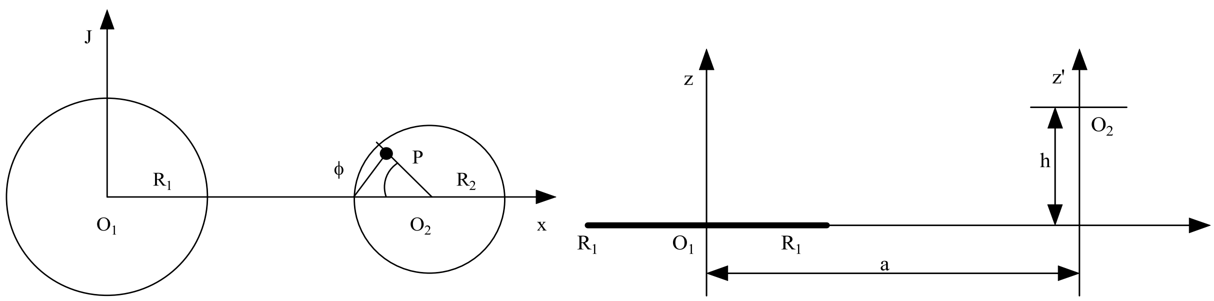

Fig. 9. Non-coaxial circular filaments.

The axial distance d is changed from 0 mm to 20 mm, while other parameters are kept constant and the air gap is fixed at 2 mm. The calculation of mutual inductance as a function of axial distance for different geometries is shown in Fig. 8.

As illustrated in Fig. 8, the calculated mutual inductance curve is compared with anthor simulated results which use concentric circles equal circular spiral wound coils [7]. As shown in Fig. 9 formula for circular filaments with parallel axes but lateral misalignment is

$$M = \frac{1}{\pi}\int_0^{\pi} \frac{fM_\gamma}{A^2} d\vartheta \tag{16}$$

Where

$$A = \sqrt{1 + \left(\frac{a}{R_2}\right)^2 - 2\frac{a}{R_2} COS\vartheta} \tag{17}$$

$$f = 1 - \frac{a}{R_2} COS\vartheta \tag{18}$$

is the mutual indutance for coaxial circular filaments (the radius of which are R_1 and) which is shown as below,

$$M_\gamma = \mu_0 \sqrt{R_1 \rho} \left[\left(\frac{2}{k} - k\right) K - \frac{2}{k} E \right] \tag{19}$$

$$K^2 = \frac{4R_1\rho}{(R_1 + \rho)^2 + x^2} \tag{20}$$

Then, the mutual inductances of coils are obtained through summing up the total partial mutual inductances.

As shown in Fig. 8, it can be seen that calculated mutual inductances with increasing number of polygon's side are approaching with the concentric circles simulated results. And with the increasing number of polygon's side, the mutual inductance changes between polygons are declined. The change between mutual inductance curves of octagon sprial coils and dodecagon sprial coils is just a little. The error between circle calculation and dodecagon sprial coils is less than 10%. At the beginning of calculation and polygon approaching curves, the two curves are almost coincident. It can be seen that polygon with certain number sides are almost to be a circle, dodecagon sprial coils are equal to the circular spiral wound coils.

Figure 10 is the mutual inductance difference as a function of axial distance which is the output of the coils on the Fig. 1. It is shown that the curve is nearly linearity. The target range of the displacement sensor on optical aperture synthesis telescope system is 20 microns. As shown in Fig. 10, coils are supposed to be positioned as d is 5 mm as the start position of sensors. In this situation, the mutual inductance difference in every 50 nm displacement is 9.1×10^{-12} H according to the calculation. So the next step of building this sensor system is to design the circuit to detect the mutual inductance difference.

4. Conclusion

In this paper, specific to the coils of inductance displacement sensor on optical aperture synthesis telescope, mutual inductance calculation based on PEEC theory is established and verified. It can quickly determine the mutual coupling of two coils on segments in dfferent relative positions. The relationship between mutual inductance and the corresponding displacement is obtained, which is used for designing the examination system.

Acknowledgments

This work was supported by the National Science Fund of China (50907032), Jiangsu science and technology office project (BE2009162, BZ2009051), and the NUAA innovation fund (Y0803-033).

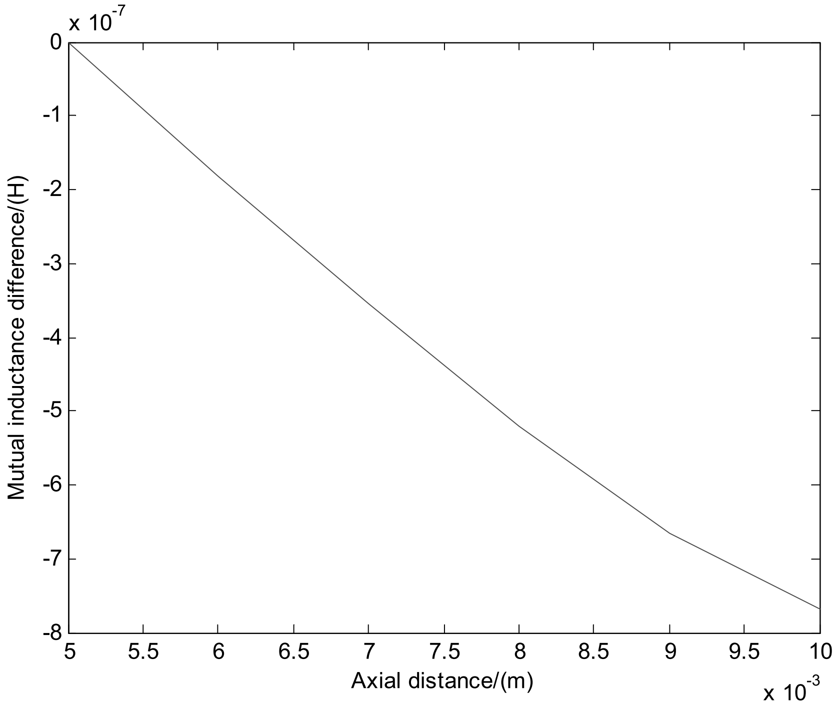

Fig. 10. Mutual inductance different as a function of axial distance.

References

[1] H. Wang, Y. Zhu, J. Cai et al., Research on the UV coverage and the optimization arrangement of the optical synthetic aperture telescope array[J], *Acta Optica Sinica* **29**(4) (2009), 1112–1116.

[2] H. Wang, Y. Zhu, J. Cai et al., Research on sub-telescopes' beams parallel and path difference adjustment to the optical aperture synthesis telescope[J], *Acta Optica Sinica* **29**(5) (2009), 1397–1402.

[3] H. Wang, Q. Luo, X. Xu et al., Three kinds of displacement sensor for segmented mirror co-focus, *Chinese Journal of Sensors and Actuators*, 2003.

[4] M.M. Colavita, A.F. Boden, S.L. Crawford et al., Keck Interferometer [C], *Proc SPIE* **3350** (1998), 776–784.

[5] W.P. Carpes, Jr., G.S. Ferreira and A. Raizer, TLM and FEM applied in the analysis of electromagnetic coupling, *IEEE Transactions on Magnets* **36**(4) (2000), 982–985.

[6] X. Zeng, J. Chen. X. Yang et al., *Mutual Inductance Coupling Research Based on PEEC Theory Inside Hybrid LPEM*, Proceedings of the CSEE, **Vol.23**(No. 7) (Jul 2004).

[7] П. Л. Калантаров, Л. А. Расчет индуктивностей слравочнаи книга,1992.

[8] Y.P. Su, X. Liu and S.Y.R. Hui, Mutual inductance calculation of movable planar coils on parallel surfaces, *2008 IEEE Power Electronics Specialists Conference* (2008), 3475–3481.